Magnetization Reversal in Ultrashort Magnetic Field Pulses

C. H. Back,[1] D. Weller,[2] J. Heidmann,[3] D. Mauri,[3] D. Guarisco,[4] E. L. Garwin,[1] and H. C. Siegmann[5]
[1]*Stanford Linear Accelerator Center, Stanford University, Stanford, California 94309*
[2]*IBM Almaden Research Center, 650 Harry Road, San Jose, California 95120*
[3]*IBM Storage Systems Division, 5600 Cottle Road, San Jose, California 95193*
[4]*Department of Materials Science Engineering, Stanford University, Stanford, California 94305*
[5]*Laboratorium für Festkörperphysik, ETH Zürich, CH-Zürich, Switzerland*
(Received 2 September 1997)

Strong in-plane magnetic field pulses of 2–4.4 ps duration are used to study magnetization reversal in perpendicularly magnetized Co/Pt films. Ring domains, reminiscent of the field contour during exposure, are observed later with Kerr microscopy. Their radii represent switching fields which are in quantitative agreement with the coherent rotation model. The observation of intrinsic transition broadening is attributed to the existence of static and dynamic fluctuations of the magnetic anisotropy. [S0031-9007(98)07344-X]

PACS numbers: 75.70.Cn, 75.10.–b, 75.40.–s

Magnetization reversal is governed by the sum of internal and external field contributions and thermal fluctuations [1,2]. A stable state is characterized by an energy minimum and reversal requires overcoming a barrier ΔE between adjacent minima by applying an external magnetic field. At nonzero temperature T, thermal fluctuations help to overcome ΔE, and thus magnetization reversal becomes temperature assisted [1,2]. Street and Wooley [3] have postulated a characteristic "wait time" τ according to $1/\tau = f_0 \exp(-\Delta E/kT)$ to account for the statistical nature of the reversal. Here $f_0 = 1/\tau_0$ is an attempt frequency which is of the order of 10^9–10^{12} s^{-1} [1,4,5] and depends in a nontrivial fashion on variables like anisotropy constant, magnetization, and damping [2–4]. In a simple approach it may be viewed as being connected to the characteristic time needed for energy exchange between lattice and spin, i.e., the spin lattice relaxation time τ_{sl} [6]. Recent experiments indicate values of $\tau_0 \cong 4 \times 10^{-9}$ s for small ferromagnetic particles [7,8] and $\tau_0 \cong 1 \times 10^{-9}$ s for particulate magnetic recording media [9]. For magnetic excitations occurring on time scales much shorter than τ_{sl} thermal activation ceases to exist, thus the motion of the magnetization vector should simply follow the Landau-Lifshitz (LL) equation. The present paper discusses an experiment allowing a systematic study of magnetization reversal at time scales below τ_{sl}. In the described experiment we apply a short but strong magnetic field pulse (in fact, the field pulse is shorter than the time scale given by the precessional frequency of the magnetic sample) in the hard plane of perpendicularly magnetized ferromagnetic films, and the evolving magnetization patterns are inspected weeks later with a Kerr microscope. In this particular geometry the resulting initial reversal occurs by precession of the magnetization while the field pulse is present. The magnetization subsequently, on a much longer time scale, relaxes into the easy magnetization direction given by the magnetic anisotropy. In this regard, the present experiment is fundamentally different from conventional magnetic writing experiments where a field is applied parallel to the anisotropy field axis and the length of a magnetic field pulse is much longer than τ_{sl}. This novel magnetic switching experiment also differs from ferromagnetic resonance (FMR) measurements where a small rf excitation causes coherent precession of the magnetic moments around a constant effective field composed of internal and external field contributions [10]. Because FMR is a stationary process it does not yield any information about the contribution of thermal activation and its variable impact on the magnetic reversal process for different excitation times. The realization of extremely short magnetic field pulses in the laboratory frame, sufficiently strong to switch the magnetization of ferromagnetic materials with large anisotropy fields, seems unfeasible. Earlier attempts to produce such fields have resulted in pulses of 50 ps duration, but with small peak amplitudes of about 10 Oe [11]. Stronger fields of up to approximately 2 kOe, but of fairly long duration of 640 ps were reached in Ref. [12]. Recently, Siegmann *et al.* [13] have demonstrated the possibility of using the finely focused 46.6 GeV electron beam in the Final Focus Test Beam (FFTB) section of the Stanford Linear Accelerator Center as a magnetic field source for pulses as short as 2–6 ps and field amplitudes up to several tesla. They already reported on magnetization reversal on picosecond time scales; however, their initial pioneering experiment suffered from rather large uncertainties in the beam parameters rendering a quantitative analysis impossible. We have repeated this experiment and are now able to give a rigorous test of the Stoner-Wohlfarth model at picosecond time scales by varying two crucial parameters: pulse duration and strength of the anisotropy field. A quantitative comparison of the observed switching radii with a LL based calculation shows that the coherent rotation model applies even for continuous highly exchange coupled ferromagnetic films. Of particular interest is the sharpness of the transition region between up and down magnetized domains: its width cannot be explained in this

model, and we postulate that the observed broadening may be related to anisotropy fluctuations. This intrinsic broadening effect poses a fundamental limitation to high data rate magnetic recording.

The polycrystalline thin film samples are e-beam evaporated $10 \times [\text{Co } x \text{ Å}/\text{Pt } 12 \text{ Å}]$ multilayers ($x = 4.4$, 4.7, 6.9, 8.9, and 9.2 Å) grown at $\cong 200\,^{\circ}\text{C}$ onto (111) textured, 200 Å thick Pt buffer layers deposited at 400 °C onto SiN_x coated Si(100) substrates. Furthermore, we include three $Co_{28}Pt_{72}$ alloy samples with thicknesses of 80, 125, and 160 Å, grown at 220 °C by coevaporation onto Pt seeded fused silica substrates, as reported earlier [13]. All samples were capped with 20 Å of Pt at ambient temperature for corrosion protection. The samples were characterized with Rutherford backscattering spectrometry and x-ray diffraction (XRD). XRD revealed strong (111) texturing. The average ($\Theta - 2\Theta$ XRD) grain size was 15 nm. Magnetic properties were established prior to the experiments by using vibrating sample and torque magnetometries as well as magneto-optic Kerr effect measurements. Most relevant in conjunction with the present discussion is the effective magnetic anisotropy field $(H_K)_{\text{eff}} = H_k - 4\pi M_s$ which may be viewed as the field needed to saturate the sample in the hard plane. $(H_K)_{\text{eff}}$ was determined within $\pm 10\%$ accuracy and ranged from 16 to 32 kOe. Coercive fields ranged between 1.3 and 3.5 kOe, ensuring that a written domain pattern can still be measured weeks after field exposure.

The experiments were performed at the focal point of the FFTB section of the Stanford Linear Accelerator as described before [13]. The premagnetized samples were stepped through the beam pipe synchronous to the 1 Hz repetition rate of the 46.6 GeV electron beam. Each sample was exposed 15 times at different locations allowing us to investigate the influence of pulse length and number of repetitions on samples with identical anisotropy. Before each run the length of the beam pulse was selected and its x and y dimensions were determined at the sample location [14]. The number of electrons per bunch was recorded on a shot to shot basis using two toroids in the beam line. The Gaussian half-widths of the electron beam in the x and y directions were determined to be $\sigma_x = 3.8 \pm 0.4$ μm and $\sigma_y = 0.8 \pm 0.2$ μm, respectively. The number of electrons per bunch was $(9.6 \pm 0.2) \times 10^9$. The temporal pulse lengths in the three experiments were 2, 3, and 4.4 ps. They were calibrated with a rather large error of about 15% by recording the synchrotron radiation in the north arc leading to the Stanford Large Detector. The magnetic field produced by the electron beam moving essentially at the speed of light is computed from the current density $j(x, y, t) = n(x, y, t)ec$ by simply applying Ampère's law. Here $n(x, y, t)$ is the number of electrons at a given position and time, determined by the three dimensional Gaussian beam. Large fields up to 20 T are reached close to the surface of the beam. Weeks after exposure the samples were retrieved from the FFTB, and the magnetic domain patterns were examined in a Kerr microscope [15]. Some samples were additionally investigated with magnetic force microscopy (MFM). Figure 1a shows a Kerr micrograph of a pattern written with a single 2 ps pulse into a Co/Pt multilayer sample with $(H_K)_{\text{eff}} = 31.9$ kOe that had been premagnetized along the $-z$ axis. Figure 1b shows a corresponding

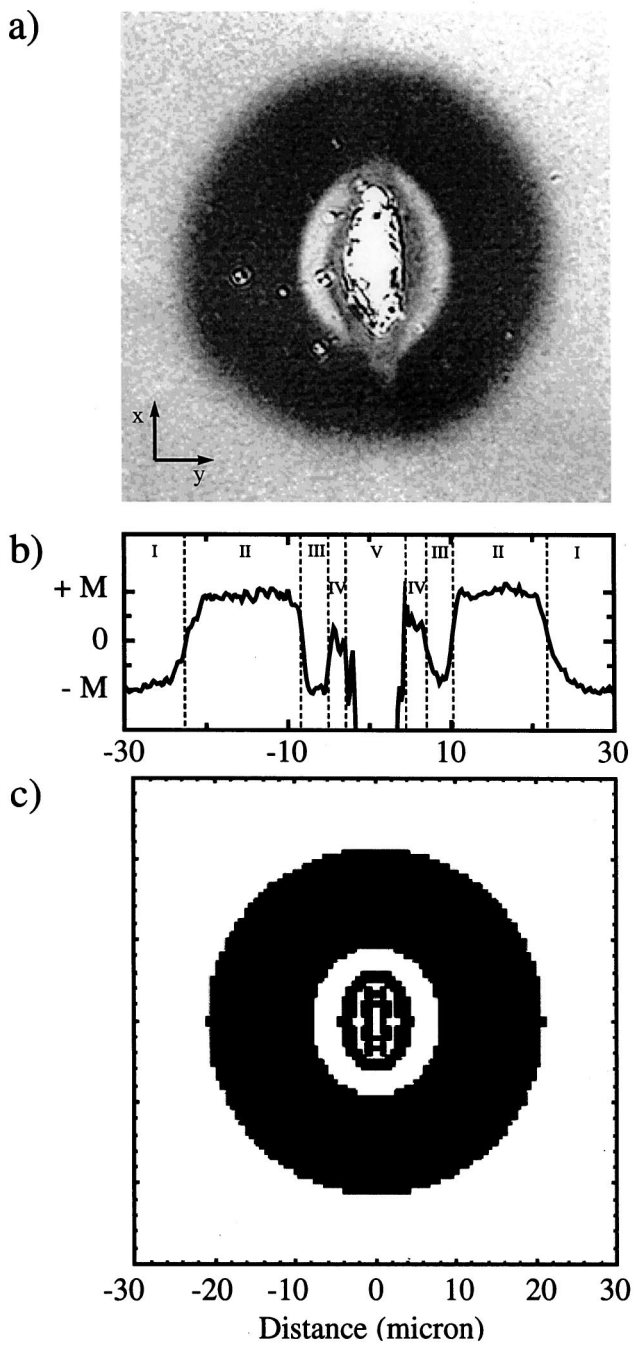

FIG. 1. (a) Domain pattern written into a Co/Pt multilayer with $(H_K)_{\text{eff}}$ of 31.9 kOe. The field pulse lasted for 2 ps. (b) Line scan along the y direction through the center of the domain. (c) Calculation of the domain pattern for the sample of (a) using the LL equation (details see text). The border lines between the up and down domains represent lines of constant magnetic field. At $t = 0$ this field amounts to 28.8 kOe for the outer transition and 69.8 kOe for the inner transition.

line scan along the y direction at $x = 0$. Clearly five regions can be distinguished. Region I far away from the center is still magnetized along its original direction represented by a white contrast and the value M in the line scan. The dark ring of region II represents an area where the magnetization has switched at a corresponding maximum magnetic field at $t = 0$ of 26.1 kOe and is now pointing along the $+z$ direction. In region III, even closer to the core of the electron beam the magnetic field pulse was strong enough $[H(t = 0) = 62.1$ kOe$]$ to cause a second reversal of the magnetization direction. This region is followed by an area with zero net magnetization—region IV—and correspondingly the contrast appears grey in the image. Region V represents the actual area of impact of the electron beam. The 46.6 GeV beam has evaporated the surface material and caused a crater of several microns depth. Region IV has been demagnetized. MFM measurements in this region indicate the presence of magnetic domains with an average size of 0.3–0.5 μm. The domains are not resolved in the shown Kerr micrograph, and thus zero net magnetization is recorded. What is the cause of the domain formation? Heating the sample above its Curie temperature of about 500 K may cause demagnetization. Less than 1% of the beam energy is dumped into the material and a cylindrical heat wave is formed around the path of the electron beam. Based on a simple heat transport calculation we conclude that the Curie temperature cannot be reached at the borderline of region IV. However, it is known that the electron beam can carry a halo of particles at very low particle density, below the detection limit of the FFTB wire scanners, which can easily account for overheating. To investigate this problem we have—in a separate experiment—exposed the same sample to a beam with the same number of electrons and the same pulse length, but with a different shape in the x-y plane. This beam was known to have a larger background level of particles. In this test exposure the size of region IV increased to the extent that region III almost completely vanished.

A simple micromagnetic model based on the LL equation is used to understand the switching behavior in regions II and III. Here a first term describes the precession of the magnetization in the magnetic field, and a second term describes the rotation of the magnetization into the direction of the field due to energy dissipation [16]. The total magnetic field is the sum of the effective anisotropy field and the beam field. Both exchange and dipolar interactions are neglected. We will see that even this simplified model can explain the basics of the switching process. The sample is subdivided into a square mesh, each cell having the same perpendicular magnetization before a Gaussian beam pulse as generated by the electron beam is applied. Figure 1c shows the calculated switching pattern for the film of Fig. 1a reproducing the observed gross features. Figure 2 summarizes calculated and measured switching radii for the set of multilayers at 2 ps pulse length. In Fig. 2a we plot switching radii versus the effective anisotropy. The experimental results agree well with the calculated values within the error bars which are mainly due to uncertainties in the pulse length. Figure 2b displays the experimental and theoretical switching radii plotted versus pulse length at fixed $(H_K)_{\text{eff}} = 16.5$ kOe. Both the first (between regions I and II) and the second (between regions II and III) switches are included. Again good agreement is found. Figure 3 summarizes measurements from different experiments using different pulse lengths, beam shapes, and thin film samples, including alloys. Plotted is the ratio of experimental and calculated switching radii. For all experiments the agreement is found to be better than 16% with the exception of the sample with the large anisotropy field of 32 kOe, where the discrepancy amounts to 40%. The agreement is in all cases within the experimental error. In the line scan in Fig. 1b one observes that the transition between the two states of magnetization is not sharp. One might think that the spreading of the domains over 5 μm in the transition region between regions I and II can be explained by a nonuniform magnetization direction. If the magnetization direction in individual cells deviates statistically from the normal direction by a few degrees, the starting condition for spin rotation in

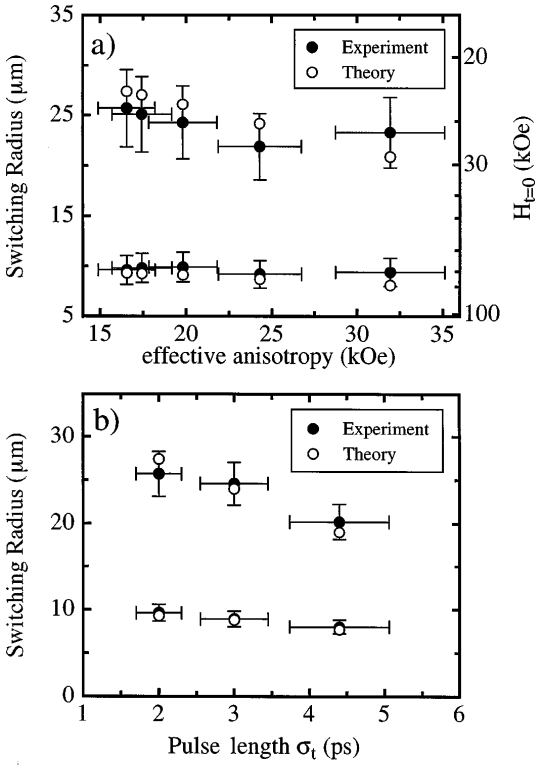

FIG. 2. (a) Measured (full circles) and calculated (open circles) switching radius in the y direction and at $x = 0$ as a function of the strength of the anisotropy field. The lower data points present data on the second switching closer to the region of impact. The axis to the right gives the corresponding magnetic field strength at $t = 0$. (b) Measured (full circles) and calculated (open circles) switching radius in the y direction and at $x = 0$ as a function of the pulse duration for a sample with $(H_K)_{\text{eff}}$ of 16.5 kOe.

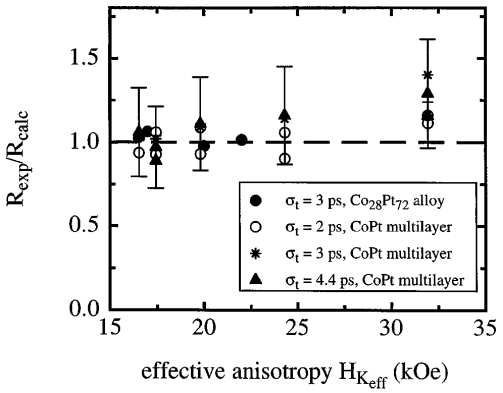

FIG. 3. Ratio of measured to calculated switching radius for all samples and all pulse durations. The broken line indicates the Stoner-Wohlfarth value of 1.

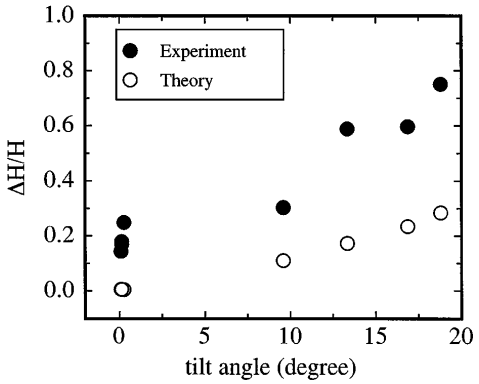

FIG. 4. Measured (full circles) and calculated (open circles) ratio of the width of the transition region to the transition radius versus the tilt angle of the magnetization direction away from the normal as deduced from the Kerr hysteresis loops.

each cell differs, and a spread over a broad transition region can be expected. An average magnetization tilt angle away from the normal direction can be deduced from the measured ratio between remanent and saturation magnetization. The transition width can then be calculated, again using the LL equation. The results are shown in Fig. 4. The calculated transitions appear much narrower than the experimentally observed ones. We consider two possible reasons based on local lattice distortions. Deviations from the ideal lattice cause local changes of the electronic band structure, which via spin orbit coupling modifies the magnetic anisotropy of a given material. For example, strain of 1% in a Co single crystal may lead to changes in the magnetic anisotropy energy of up to 60%. Locally lattice strain can be caused by two mechanisms: (i) Local lattice imperfections caused by imperfect growth and (ii) at the time of the magnetic field excitation the lattice is frozen into a phonon distorted state. We can use the Debye Waller factor to approximate the magnitude of the lattice distortions caused by temperature to 5%. From our XRD measurements we conclude that the sum of static and dynamic distortions is of the order of 10%–15%, thus static distortions are of the same magnitude or larger than dynamic distortions. Both effects lead to a distribution of initial states before the magnetic field pulse acts on the sample, and this in turn results in a distribution of small up and down domains after the field pulse has passed. On a much longer time scale these domains then relax into domains of at least the size of the exchange length. This relaxation process does not affect the written domain pattern, but only the size of the domains in the transition region.

In conclusion, we have shown that magnetic switching in perpendicular magnetized samples at ultrashort time scales can be well understood within the simple LL model. We have shown that the width of the written transitions is not only determined by the quality of the magnetic material, but is ultimately determined by intrinsic physical properties such as phonons. A phonon driven broadening of the transition region would hint to the ultimate limit of transition density for ultrafast magnetic recording.

We thank D. W. G. S. Leith and D. L. Burke for supporting this project. We gratefully acknowledge the input of a number of people at the FFTB and PEL, particularly C. Bula, G. J. Collet, C. Field, and F. King. We thank M. Best for the AFM/MFM work. C. H. B. gratefully acknowledges the Swiss National Fund for financial support. This work was supported in part by the Department of Energy under Contract No. DE-AC03-76SF00515.

[1] L. Néel, Ann. Geophys. **5**, 99 (1949).
[2] W. F. Brown, Phys. Rev. **130**, 1677 (1963).
[3] R. Street and J. C. Wooley, Proc. Phys. Soc. London Sect. A **62**, 562 (1949).
[4] P. Gaunt, J. Appl. Phys. **48**, 3470 (1977).
[5] A. Lyberatos and R. W. Chantrell, J. Phys. Condens. Matter **9**, 2623 (1997).
[6] Values for τ_{sl} are found to lie in the 100 ps range. A. Vaterlaus *et al.,* Phys. Rev. B **46**, 5280 (1992); A. Scholl *et al.*, Phys. Rev. Lett. **79**, 5146 (1997), and references therein.
[7] W. Wernsdorfer *et al.,* Phys. Rev. Lett. **78**, 1791 (1997).
[8] M. Ledermann, S. Schultz, and M. Ozaki, Phys. Rev. Lett. **73**, 1986 (1994).
[9] L. He *et al.,* J. Magn. Magn. Mater. **155**, 6 (1996).
[10] George T. Rado, J. Appl. Phys., Suppl. **32**, No. (3), 129 (1960).
[11] M. Freemann *et al.,* IEEE Trans. Magn. **27**, 4840 (1991).
[12] W. D. Doyle, L. He, and P. J. Flanders, IEEE Trans. Magn. **29**, 3634 (1993).
[13] H. C. Siegmann *et al.,* J. Magn. Magn. Mater. **151**, L8 (1995).
[14] C. Field, Nucl. Instrum. Methods Phys. Res., Sect. A **360**, 467 (1995).
[15] W. Rave, R. Schaefer, and A. Hubert, J. Magn. Magn. Mater. **65**, 7 (1987).
[16] The damping parameter α is assumed to be 0.1. However, switching occurs in the initial 2–4 ps when the field is applied. At these time scales it has been shown that the actual choice of α is not critical: L. He and W. D. Doyle, J. Appl. Phys. **79**, 6489 (1996).